J. Fluid Mech. (1991), *vol.* 224, *pp.* 625–644
Printed in Great Britain

Reflection and transmission from porous structures under oblique wave attack

By ROBERT A. DALRYMPLE[1], MIGUEL A. LOSADA[2] AND P. A. MARTIN[3]

[1] Center for Applied Coastal Research, Department of Civil Engineering, University of Delaware, Newark, DE 19716, USA

[2] Departamento de Ciencias y Técnicas del Agua y del Medio Ambiente, University of Cantabria, Santander, Spain

[3] Department of Mathematics, University of Manchester, Manchester M13 9PL, UK

(Received 23 January 1990)

The linear theory for water waves impinging obliquely on a vertically sided porous structure is examined. For normal wave incidence, the reflection and transmission from a porous breakwater has been studied many times using eigenfunction expansions in the water region in front of the structure, within the porous medium, and behind the structure in the down-wave water region. For oblique wave incidence, the reflection and transmission coefficients are significantly altered and they are calculated here.

Using a plane-wave assumption, which involves neglecting the evanescent eigenmodes that exist near the structure boundaries (to satisfy matching conditions), the problem can be reduced from a matrix problem to one which is analytic. The plane-wave approximation provides an adequate solution for the case where the damping within the structure is not too great.

An important parameter in this problem is $\Gamma_2 = \omega^2 h(s - \mathrm{i}f)/g$, where ω is the wave angular frequency, h the constant water depth, g the acceleration due to gravity, and s and f are parameters describing the porous medium. As the friction in the porous medium, f, becomes non-zero, the eigenfunctions differ from those in the fluid regions, largely owing to the change in the modal wavenumbers, which depend on Γ_2.

For an infinite number of values of Γ_2, there are no eigenfunction expansions in the porous medium, owing to the coalescence of two of the wavenumbers. These cases are shown to result in a non-separable mathematical problem and the appropriate wave modes are determined. As the two wavenumbers approach the critical value of Γ_2, it is shown that the wave modes can swap their identity.

1. Introduction

Porous structures, such as rubble-mound breakwaters, are used to protect harbours, inlets, and beaches from wave action. Further, they are often used as absorbers in laboratories to remove unwanted waves during experiments. The functional efficiency of these structures is evaluated for vertically sided structures by calculating the reflection and transmission of waves. The reflection and transmission coefficients depend on the characteristics of the waves (wave height, H, wave period, T, and angle of incidence, θ) and of the structure (such as its geometry and its composition).

Theoretical solutions for the reflection and transmission coefficients for porous structures have been derived previously by several authors, using eigenfunction expansions in the fluid and in the porous medium. The existing solutions are valid for structures with rectangular cross-sections under normally incident linear waves. Dissipation of energy inside the structures is taken into account through a linearized friction term, involving a friction coefficient, f, which is evaluated by fulfilling Lorentz's condition of equivalent work (Sollitt & Cross 1972; O. Madsen 1974; O. Madsen & White 1976; P. Madsen 1983; and others). These models have been reasonably verified in laboratory experiments.

Trapezoidal breakwaters have been analysed by considering an equivalent breakwater of rectangular cross-section (Sollitt & Cross 1972) or through boundary-element models (Sulisz 1985). An additional dissipation of energy may be included in order to evaluate wave breaking on the slope (Sollitt & Cross 1972; O. Madsen & White 1976). Further, several laboratory studies have been conducted to investigate the reflected and transmitted waves for specific types of permeable structures under normally incident waves (Iwasaki & Numata 1970; Dattatri, Raman & Shankar 1978).

In this paper the theory of wave transmission and reflection by an infinitely long, homogeneous porous structure is extended to the case of linear waves at oblique incidence, providing the basis for treating an incident directional spectrum. Further, a plane-wave approximation, which neglects the evanescent wave modes, is given for several geometries. It will be shown that for almost all the practical cases, the plane-wave approximation, which has the long-wave solution as a special case, is sufficient to describe the wave behaviour, thus providing a far simpler solution technique. This plane-wave analysis has analogues in other fields of physics, for example, the transmission and reflection of plane acoustic waves by a porous medium (e.g. Morse & Ingard 1968, §6.3) or of TM electromagnetic waves by a conducting surface (e.g. Yeh 1988).

For a given structure, there may be a large number of wave conditions for which the eigenfunction approach, based on the Sturm–Liouville theory, is no longer applicable. These cases correspond to the situation when two eigenfunctions have the same eigenvalue (wavenumber). We show that for this case the boundary-value problem is no longer separable and must be treated by a Green's-function analysis. In acoustics, this phenomenon has been observed by Tester (1973), who examined the attenuation of acoustic waves in rectangular ducts, with absorbing sides. He showed that this new wave mode varies linearly with propagation distance, but in fact is the most rapidly decaying of all the modes in the problem.

The approach we follow is to present the coupled boundary-value problem and the matching conditions between the fluid and porous medium; then the full eigenfunction solution is examined. In §4, the plane-wave approximations are developed for several structure geometries. In §5, the cases where the modal wavenumbers coalesce and mode swapping occurs are discussed and the solution for these special cases is presented. Finally, results from the full eigenfunction solution and the plane-wave approximation are presented and compared.

2. Theoretical formulation

We consider the interaction of a gravity wave train with a single homogeneous, isotropic, porous structure of width b between two semi-infinite fluid regions of constant depth, h, as shown in figure 1. The obliquely incident wave train

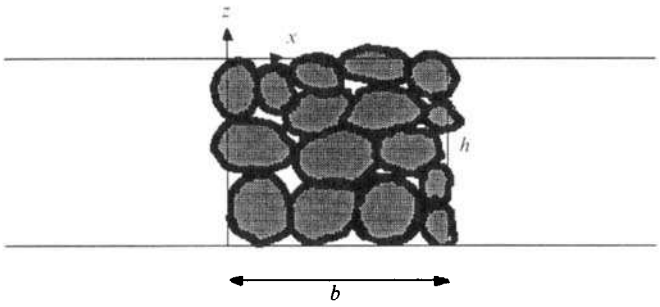

FIGURE 1. Schematic diagram.

encountering the breakwater face is partially reflected and partially transmitted. The wave motion inside the porous structure decays as it propagates through the pores. Then, as it encounters the leeward breakwater face, it is partially reflected back into the structure and partially transmitted into the leeward semi-infinite fluid region. Inside the breakwater, the transmitted and reflected waves are subsequently reflected and transmitted back and forth between the two outside faces.

For an incompressible fluid and irrotational motion, the wave field outside the structure can be specified by velocity potentials: Φ_1 in the seaward region (denoted region 1) and Φ_3 in the leeward region of the breakwater (region 3). The linear boundary-value problem for water of constant depth h is well known.

In the rigid porous medium, region 2, the incompressible fluid motion for the discharge velocity (flow per unit area) is also describable by a potential and a modified free-surface boundary condition. These equations have been derived by Sollitt & Cross (1972) and are provided for completeness in Appendix A. Characteristics of the porous medium are its porosity, ϵ, the linear friction factor, f, and the inertial term, s, which are taken to be constant here. For all computations in this paper, $\epsilon = 0.4$ and $s = 1$.

The boundary-value problem can be completely solved if the potential $\Phi_i(x, y, z, t)$ is known in the ith region, where $i = 1, 2, 3$. We suppose that a wave, travelling at an angle θ to the x-axis, is incident on the breakwater, which lies along the y-axis. Then, we can write

$$\Phi_i(x, y, z, t) = \mathrm{Re}\,[\phi_i(x, z)\,\mathrm{e}^{-\mathrm{i}(\lambda y - \omega t)}], \quad i = 1, 2, 3, \tag{2.1}$$

where the parameter λ is related to the progressive mode wavenumber k_0 by the angle of incidence, $k_0 \sin\theta = \lambda$. (To satisfy the matching conditions at each vertical interface, the y-variation of the solution in each region must be the same (Snell's law)). The potentials ϕ_i must satisfy the following boundary-value problems.

In region i:

$$\left.\begin{aligned} \frac{\partial^2\phi_i}{\partial x^2} + \frac{\partial^2\phi_i}{\partial z^2} - \lambda^2\phi_i = 0, \quad -h \leqslant z \leqslant 0, \\ \frac{\partial\phi_i}{\partial z} = 0 \quad \text{at} \quad z = -h, \\ \frac{\partial\phi_i}{\partial z} - \frac{\Gamma_i}{h}\phi_i = 0 \quad \text{at} \quad z = 0, \end{aligned}\right\} \tag{2.2}$$

where $\Gamma_1 = \Gamma_3 = \omega^2 h/g$ and $\Gamma_2 = \omega^2 h(s - \mathrm{i}f)/g$.

Since the solutions in adjacent regions must be continuous at each interface, continuity of mass flux and pressure at $x = 0$ (between regions 1 and 2) and at $x = b$ (between regions 2 and 3) is required.

At $x = 0$,

$$\left.\begin{aligned} \phi_{1x} &= \epsilon\phi_{2x}, \\ \phi_1 &= (s-\mathrm{i}f)\,\phi_2; \end{aligned}\right\} \tag{2.3}$$

at $x = b$,

$$\left.\begin{aligned} \epsilon\phi_{2x} &= \phi_{3x}, \\ (s-\mathrm{i}f)\,\phi_2 &= \phi_3, \end{aligned}\right\} \tag{2.4}$$

where the subscript indicates derivative with respect to the variable, x.

3. Full solution

In region 1, the function ϕ_1, by separation of variables, is

$$\phi_1(x,z) = I_0(z)\{\exp[-\mathrm{i}x(k_0^2-\lambda^2)^{\frac{1}{2}}] + R\exp[\mathrm{i}x(k_0^2-\lambda^2)^{\frac{1}{2}}]\} + \sum_{n=1}^{\infty} I_n(z)\,R_n\exp[\mathrm{i}x(k_n^2-\lambda^2)^{\frac{1}{2}}], \tag{3.1}$$

where a family of evanescent modes is included to satisfy the matching conditions at the porous structure; here, and below, we choose the branch of the square root that satisfies

$$\mathrm{Re}\{(k^2-\lambda^2)^{\frac{1}{2}}\} \geqslant 0 \quad \text{and} \quad \mathrm{Im}\{(k^2-\lambda^2)^{\frac{1}{2}}\} \leqslant 0. \tag{3.2}$$

Note that the subscript zero refers to the incident and reflected waves whereas the subscripts, $n > 0$, refer to the evanescent modes. $R\,(\equiv R_0)$ is the reflection coefficient and is a complex quantity.

The depth dependency of the problem is provided by the $I_n(z)$, which are given by

$$I_n = \frac{\mathrm{i}g}{\omega}\frac{\cosh k_n(h+z)}{\cosh k_n h}, \quad n = 0,1,2,\ldots, \tag{3.3}$$

and the k_n satisfy the linear dispersion relation

$$\Gamma_1 = k_n h\tanh k_n h, \quad n = 0,1,2,\ldots. \tag{3.4}$$

This transcendental equation has real roots $\pm k_0$, where $k_0 > 0$, and an infinite number of purely imaginary roots.

It is well known that the set of eigenfunctions, $\{\cosh k_n(h+z),\ n = 0,1,2,\ldots\}$, is a complete orthogonal set, with

$$\int_{-h}^{0} \cosh k_n(h+z)\cosh k_m(h+z)\,\mathrm{d}z = \delta_{nm}N^2, \tag{3.5}$$

where

$$N^2(k_n) = \frac{\sinh 2k_n h + 2k_n h}{4k_n}. \tag{3.6}$$

In region 2, the velocity potential is given by

$$\phi_2 = \sum_{n=1}^{\infty} P_n(z)\{A_n\exp[-\mathrm{i}x(K_n^2-\lambda^2)^{\frac{1}{2}}] + B_n\exp[\mathrm{i}(x-b)\,(K_n^2-\lambda^2)^{\frac{1}{2}}]\}, \tag{3.7}$$

where the depth dependency is now

$$P_n(z) = \frac{\mathrm{i}g}{\omega}\frac{\cosh K_n(h+z)}{\cosh K_n h}, \quad n = 1,2,\ldots. \tag{3.8}$$

A_n and B_n are the complex amplitudes of the waves inside the porous structure and K_n satisfies the complex dispersion relation

$$\Gamma_2 = \Gamma_1(s-\mathrm{i}f) = \frac{\omega^2 h(s-\mathrm{i}f)}{g} = K_n h \tanh K_n h, \quad n = 1, 2, \ldots. \tag{3.9}$$

The eigenfunctions, $\{\cosh K_n(h+z),\ n = 1, 2, \ldots\}$ are also an orthogonal set of functions with the normalization factor, $N^2(K_n)$. However, under certain circumstances discussed later in §5, the expansion (3.7) may be incomplete and an additional non-separable mode must be introduced.

Finally, in region 3 the function ϕ_3 should be

$$\phi_3 = TI_0(z)\exp[-\mathrm{i}(x-b)(k_0^2-\lambda^2)^{\frac{1}{2}}] + \sum_{n=1}^{\infty} T_n I_n(z)\exp[-\mathrm{i}(x-b)(k_n^2-\lambda^2)^{\frac{1}{2}}], \tag{3.10}$$

where I_0 and I_n are defined as before in (3.3), $T(\equiv T_0)$ is the (complex) transmission coefficient and $T_n, n > 0$, are the complex amplitudes of the family of evanescent modes present at the leeward interface. Furthermore, k_0 and k_n also satisfy (3.4) as the depth is constant in all regions.

Substituting ϕ_1, ϕ_2 and ϕ_3 into (2.3) and (2.4) in order to match the solutions at the interfaces, $x = 0$ and $x = b$, a system of equations in R, R_n, T, T_n, A_n and B_n is obtained. To simplify the solution of the large system, some algebraic manipulation is done. First, the orthogonality of the P_n series over the depth domain $(-h, 0)$ is used, resulting in a new system of equations in A_m and B_m. Next A_m and B_m are eliminated from this system of equations, giving a system of coupled equations in R, $T(\equiv T_0)$, R_n, and $T_n, n > 0$:

$$\left.\begin{aligned}
&\sum_{n=0}^{\infty} \frac{X_{n,m}}{X_{0,m}} R_n\left(M_n + \frac{\epsilon}{s-\mathrm{i}f}\mathscr{M}_m\right) + E_m^- \sum_{n=0}^{\infty} \frac{X_{n,m}}{X_{0,m}} T_n\left(M_n - \frac{\epsilon}{s-\mathrm{i}f}\mathscr{M}_m\right) = 1 - \frac{\epsilon}{s-\mathrm{i}f}\mathscr{M}_m,\\
&\sum_{n=0}^{\infty} \frac{X_{n,m}}{X_{0,m}} R_n\left(M_n - \frac{\epsilon}{s-\mathrm{i}f}\mathscr{M}_m\right) + E_m^+ \sum_{n=0}^{\infty} \frac{X_{n,m}}{X_{0,m}} T_n\left(M_n + \frac{\epsilon}{s-\mathrm{i}f}\mathscr{M}_m\right) = 1 + \frac{\epsilon}{s-\mathrm{i}f}\mathscr{M}_m
\end{aligned}\right\} \tag{3.11}$$

for $m = 1, 2, \ldots$, where the following definitions have been adopted:

$$\left.\begin{aligned}
\mathscr{M}_m &= \left(\frac{K_m^2-\lambda^2}{k_0^2-\lambda^2}\right)^{\frac{1}{2}}, \quad M_n = \left(\frac{k_n^2-\lambda^2}{k_0^2-\lambda^2}\right)^{\frac{1}{2}},\\
E_m^{\pm} &= \exp[\pm \mathrm{i}b(K_m^2-\lambda^2)^{\frac{1}{2}}],\\
X_{n,m} &= \int_{-h}^{0} I_n P_m \,\mathrm{d}z = -\frac{g(s-\mathrm{i}f-1)}{(s-\mathrm{i}f)(K_m^2-k_n^2)}.
\end{aligned}\right\} \tag{3.12}$$

It is straightforward to show that (3.11) transforms into equations given by Sollitt & Cross (1972, p. 1837) for the normal incidence case (except for a misprint in E_m in the second equation where the negative sign should be a plus). Once R_n and T_n have been evaluated, A_m and B_m can be calculated from

$$\left.\begin{aligned}
A_m &= \frac{1}{2\epsilon X_{m,m}(s-\mathrm{i}f)}\left[\sum_{n=0}^{\infty} X_{n,m} R_n\left(\epsilon - \frac{M_n}{\mathscr{M}_m}(s-\mathrm{i}f)\right) + X_0\left(\epsilon + \frac{s-\mathrm{i}f}{\mathscr{M}_m}\right)\right],\\
B_m &= \frac{1}{2\epsilon X_{m,m}(s-\mathrm{i}f)}\sum_{n=0}^{\infty} X_{n,m} T_n\left(\epsilon - \frac{M_n}{\mathscr{M}_m}(s-\mathrm{i}f)\right).
\end{aligned}\right\} \tag{3.13}$$

In practice, the infinite summations in (3.11) and (3.13) must be truncated to a finite number of terms.

4. Plane-wave approximations

In the plane-wave assumption, only the most progressive mode (least damped) of all the modes in each region is used in satisfying the matching condition. For small f, the only wavenumbers used in the problem are $k = k_0$ and $K = K_1$, obtained from (3.4) and (3.9). Clearly this leads to a great simplification of the mathematics; however, significant problems can arise if K_1 is not the most progressive mode (cf. §5.2 for large f).

4.1. *Rectangular breakwater*

Inside the structure of width b, only a transmitted wave at $x = 0$ and a reflected wave at $x = b$ have to be considered. Then the velocity potentials in each region simplify to

$$\left.\begin{aligned}
\phi_1 &= I_0\{\exp[-\mathrm{i}x(k^2-\lambda^2)^{\frac{1}{2}}]+R\exp[\mathrm{i}x(k^2-\lambda^2)^{\frac{1}{2}}]\},\\
\phi_2 &= P_1\{A_1\exp[-\mathrm{i}x(K^2-\lambda^2)^{\frac{1}{2}}]+B_1\exp[\mathrm{i}(x-b)(K^2-\lambda^2)^{\frac{1}{2}}]\},\\
\phi_3 &= I_0 T\exp[-\mathrm{i}(x-b)(k^2-\lambda^2)^{\frac{1}{2}}].
\end{aligned}\right\} \tag{4.1}$$

Following the same procedure as before, the following solutions are obtained:

$$\left.\begin{aligned}
R &= \frac{\mathrm{i}(1-m^2)\sin[(K^2-\lambda^2)^{\frac{1}{2}}b]}{2m\cos[(K^2-\lambda^2)^{\frac{1}{2}}b]+\mathrm{i}(1+m^2)\sin[(K^2-\lambda^2)^{\frac{1}{2}}b]},\\
T &= \frac{2m}{2m\cos[(K^2-\lambda^2)^{\frac{1}{2}}b]+\mathrm{i}(1+m^2)\sin[(K^2-\lambda^2)^{\frac{1}{2}}b]},\\
A_1 &= \frac{T}{2E(s-\mathrm{i}f)}\frac{\Gamma}{\chi}\left[1+\frac{1}{m}\right], \quad B_1 = \frac{T}{2E(s-\mathrm{i}f)}\frac{\Gamma}{\chi}\left[1-\frac{1}{m}\right],
\end{aligned}\right\} \tag{4.2}$$

where

$$\left.\begin{aligned}
\Gamma &= \int_{-h}^{0} I_0^2\,\mathrm{d}z, \quad \chi = \int_{-h}^{0} I_0 P_1\,\mathrm{d}z,\\
E &= \exp[-\mathrm{i}b(K^2-\lambda^2)^{\frac{1}{2}}], \quad m = \frac{\epsilon}{s-\mathrm{i}f}\left(\frac{K^2-\lambda^2}{k^2-\lambda^2}\right)^{\frac{1}{2}}.
\end{aligned}\right\} \tag{4.3}$$

R and T are functions of only two parameters: m, the dimensionless admittance of the breakwater and $b(K^2-\lambda^2)^{\frac{1}{2}}$, a dimensionless width of the structure. The admittance m is defined as the ratio of the normal velocity at the breakwater to the pressure at the wall and is a measure of the hydraulic characteristics of the structure and the angle of incidence. Note that as m^2 approaches unity, then the reflection goes to zero (independently of b).

4.2. *Long-wave approximation for rectangular breakwater*

For this case, which is the shallow-water limit of the plane-wave approximation, no evanescent modes are needed in order to match the solutions between regions as the horizontal velocity of linear long waves is uniformly distributed over the vertical. The system of equations for this case is exactly the same as for plane waves; however, the values of K and k can now be obtained from the asymptotic approximation to the dispersion relations in §3:

$$\omega^2 = gk^2h, \quad \omega^2(s-\mathrm{i}f) = gK^2h. \tag{4.4}$$

R, T, A_1 and B_1 are as given by (4.2). To obtain the long-wave solutions of Sollitt & Cross (1972) and O. Madsen (1974), it is necessary to assume normal wave incidence, $\lambda = 0$, and that the breakwater is short compared to a wavelength, $kb \ll 1$. For

oblique incidence, when $m^2 \ll 1$ we obtain the following approximations for the reflection and transmission coefficients:

$$R = \frac{\mathrm{i}\Lambda}{1+\mathrm{i}\Lambda}, \tag{4.5}$$

$$T = \frac{1}{1+\mathrm{i}\Lambda}, \tag{4.6}$$

where $\Lambda \equiv b(K^2-\lambda^2)^{\frac{1}{2}}/2m$.

4.3. *Semi-infinite porous breakwater*

For this case, there are neither transmitted waves nor reflected waves inside the breakwater at $x = b$, where $b \to \infty$; that is, $T = B_1 = 0$. By fulfilling the matching conditions at $x = 0$, a system of two equations with two unknowns, R and A_1, is obtained. Solving, we obtain from the plane-wave approximation:

$$\left.\begin{aligned} R &= \frac{1-m}{1+m}, \\ A_1 &= \frac{2(\Gamma/\chi)}{(s-\mathrm{i}f)(1+m)}. \end{aligned}\right\} \tag{4.7}$$

The symbols are defined as in (4.3). This solution has a minimum at $m = 1$.

4.4. *Finite breakwater backed by an impermeable wall*

For this case, the breakwater is limited in width by an impermeable vertical wall at $x = b$. This case has been analysed by P. Madsen (1983) for long waves at normal incidence; it may represent the seaward half of a vertical mound breakwater with an impermeable core or a wave absorber in a laboratory wave tank placed next to a wall. With the plane-wave approximation, the velocity potentials are

$$\left.\begin{aligned} \phi_1 &= I_0\{\exp[-\mathrm{i}x(k^2-\lambda^2)^{\frac{1}{2}}] + R\exp[\mathrm{i}x(k^2-\lambda^2)^{\frac{1}{2}}]\}, \\ \phi_2 &= P_1\{A_1\exp[-\mathrm{i}x(K^2-\lambda^2)^{\frac{1}{2}}] + B_1\exp[\mathrm{i}(x-b)(K^2-\lambda^2)^{\frac{1}{2}}]\}, \\ \phi_3 &= 0. \end{aligned}\right\} \tag{4.8}$$

The matching conditions between regions 1 and 2 remain the same as before, while at $x = b$

$$\phi_{2x} = 0. \tag{4.9}$$

Substituting the potentials into the matching conditions and using the orthogonality relationships yields

$$\left.\begin{aligned} R &= \frac{\cos[(K^2-\lambda^2)^{\frac{1}{2}}b] - \mathrm{i}m\sin[(K^2-\lambda^2)^{\frac{1}{2}}b]}{\cos[(K^2-\lambda^2)^{\frac{1}{2}}b] + \mathrm{i}m\sin[(K^2-\lambda^2)^{\frac{1}{2}}b]}, \\ \text{where} \qquad m &= \frac{\epsilon}{s-\mathrm{i}f}\left(\frac{K^2-\lambda^2}{k^2-\lambda^2}\right)^{\frac{1}{2}}, \end{aligned}\right\} \tag{4.10}$$

which can be transformed into

$$R = \frac{1-m\left(\dfrac{1-E^2}{1+E^2}\right)}{1+m\left(\dfrac{1-E^2}{1+E^2}\right)}. \tag{4.11}$$

In order to compare this solution with Madsen's solution for normal incidence, let $\lambda = 0$ and let K and k be obtained from the long-wave forms of the linear dispersion relations (4.4). Introducing these values into the expression for m, the following new definition is obtained:

$$m = \frac{\epsilon}{s - \mathrm{i}f}\left(\frac{K}{k}\right) = \frac{\epsilon}{(s-\mathrm{i}f)^{\frac{1}{2}}} \tag{4.12}$$

which coincides with equation 4 of Madsen. Finally, (4.11) becomes

$$R = \frac{1-m+(1+m)\,\mathrm{e}^{-2\mathrm{i}kb}}{1+m+(1-m)\,\mathrm{e}^{-2\mathrm{i}kb}}, \tag{4.13}$$

which is the result obtained by Madsen (his equation 13).

5. Wavenumbers and mode swapping

Solutions of the dispersion relation within the porous medium, (3.9), as a function of Γ_2, which are necessary for both models, are obtained primarily by a Newton–Raphson procedure. For large values of the parameter f, it is important that good starting values are used. This is particularly true when the wavenumbers of two different modes are close together (or when they coincide).

5.1. *Small f*

For very small values of f and for $s = 1$, approximate values for K_n can be obtained using the k_n obtained in the water region. Define $D(K)$ as

$$D(K_{n+1}) = K_{n+1} h \sinh K_{n+1} h - \Gamma_2 \cosh K_{n+1} h, \tag{5.1}$$

such that $D(K_{n+1}) = 0$ for a solution. Expanding about the $f = 0$ solution, k_n, which is equal to one of the solutions in the water domain from (3.4), for K_{n+1} we obtain

$$D(K_{n+1}) = D(k_n) + D'(k_n)(K_{n+1} - k_n) + \tfrac{1}{2}D''(k_n)(K_{n+1} - k_n)^2 + \ldots, \tag{5.2}$$

where the primes denote differentiation with respect to k_n. To first order in $(K_{n+1} - k_n)$, we have

$$K_{n+1} \approx k_n - \frac{D(k_n)}{D'(k_n)}, \tag{5.3}$$

where

$$D(k_n) = \mathrm{i}f\Gamma_1 \cosh k_n h, \tag{5.4}$$

$$D'(k_n) = h(\sinh k_n h + k_n h \operatorname{sech} k_n h). \tag{5.5}$$

The first mode, K_1, is real for $f = 0$, corresponding to a progressive wave in the water region (k_0), and (for small f) it is the most progressive mode in the porous medium. The other modes, $K_n, n = 2, 3, \ldots$, are purely imaginary for $f = 0$. From (5.3), the influence of the f is to damp the wave motion by adding (only) an imaginary part to K_1 and real parts to the $K_n, n > 1$.

A higher-order approximation for K_n follows by substituting (5.3) for one of the $(K_{n+1} - k_n)$ in the last term of (5.2) and solving to obtain

$$K_{n+1} = k_n - \frac{D(k_n)}{\left(D'(k_n) - \dfrac{D(k_n)D''(k_n)}{2D'(k_n)}\right)}, \tag{5.6}$$

where

$$D''(k_n) = 2h^2 \cosh k_n h.$$

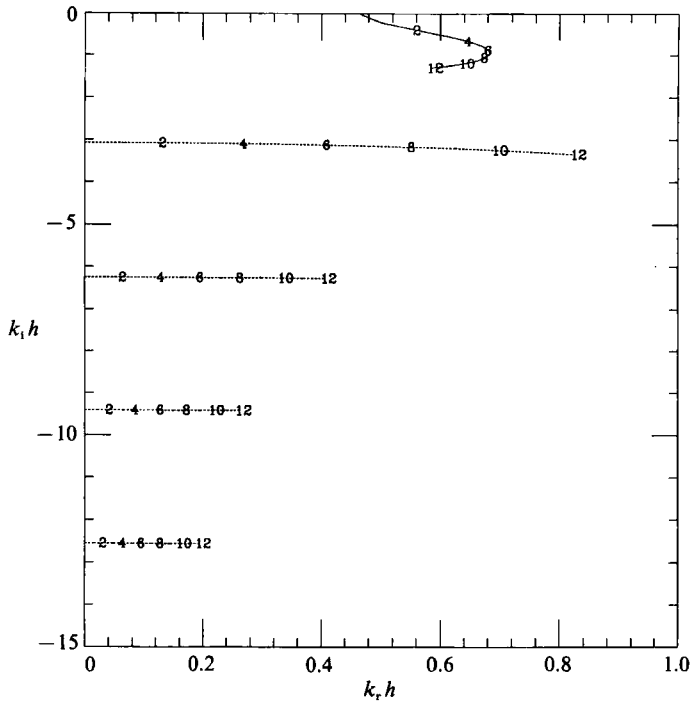

FIGURE 2. First five wavenumbers in the porous medium as the friction factor, f, varies from 0 to 12, for $\Gamma_1 = 0.2012$. Solid line corresponds to K_1; dashed lines correspond to K_n, $n = 2$–5.

For the wavenumber corresponding to k_0, this more accurate approximation now results in a change in the real part of K_1, which changes the wavelength of this mode. For a dimensionless water depth $\Gamma_1 > 1$, the wavelength of this mode is lengthened; the opposite is true for $\Gamma_1 < 1$.

Both of these approximate solutions, valid for small f, also provide a first approximation for K_n in a Newton–Raphson numerical solution procedure for larger values of f. This does not always result in a successful search for each of the infinite number of modes. Often, for large values of f, the starting value in the Newton–Raphson procedure is taken as a K_n value for a slightly smaller value of f.

5.2. *Mode swapping*

Unnoticed by previous investigators, the Newton–Raphson procedure, based on iterating (5.3), fails when $D'(K_n)$ is equal to zero. At these K_n values, the eigenfunction expansion in the porous medium also fails, since for this value the normalization parameter, $N^2(K_n)$ is equal to zero. An entirely new solution procedure is needed for these situations.

Figures 2–6 illustrate the behaviour of the dispersion relationship with dimensionless depth and the situations where the eigenfunction solution fails. The plots show the complex wavenumber for the first five non-dimensional modes ($K_n h, n =$ 1–5) for various values of f and a given value of Γ_1. To help identify the individual roots: $K_1 h$ is the upper-most curve in each figure, with the largest real part for $f = 0$; the $K_n h, n = 2$–5 are ranked from smallest to largest imaginary part for $f = 0$.

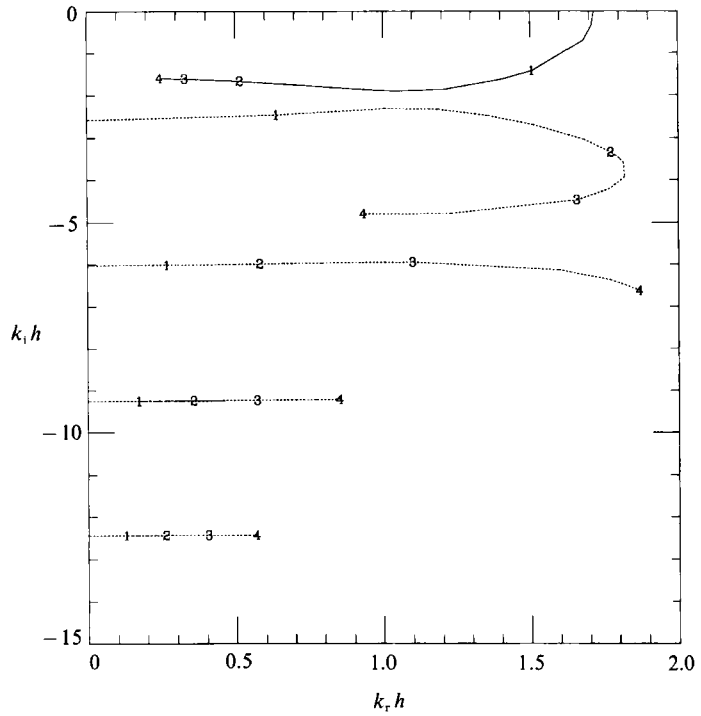

FIGURE 3. First five wavenumbers in the porous medium as the friction factor, f, varies from 0 to 4, for $\Gamma_1 = 1.6010$. Solid line corresponds to K_1.

For a shallow-water case, $\Gamma_1 = 0.2012$, figure 2 shows the dimensionless wavenumbers in the porous medium as f varies from 0 to 12. For this case, $\mathrm{Re}\{K_1\}$ first increases (as predicted by (5.6)), then decreases with f. $\mathrm{Re}\{K_2\}$ exceeds $\mathrm{Re}\{K_1\}$ for $f > 10$, which means that the plane-wave approximation is not valid for large values of f. No mode swapping appears for shallow water.

In figure 3, a value of Γ_1 much greater than unity is used (1.610) and K_1 has an immediate decrease in magnitude as f increases. For this Γ_1, K_2 is greater than K_1 for relatively small values of f.

For the value of $\Gamma_1 = 1.65061$, corresponding to intermediate water depth, the curve of $K_1 h$ versus f osculates with that of $K_2 h$, as shown in figure 4 at $K_1 h = (1.12536, -2.10620)$, corresponding to an f-value of 1.24801. For slightly smaller values of Γ_1 the dimensionless K_1 curve passes above the K_2 curve. For a slightly greater value, the K_1 curve passes below the K_2 curve; in fact, the trajectory followed by each curve is the same as that followed by the other mode at the slightly smaller value of Γ_1. This is referred to as mode swapping (e.g. Craik 1985).

As Γ_1 increases towards deeper water conditions, the dimensionless K_1 curve may intersect other higher K_n modes. Figures 5 and 6 show the double roots of $K_1 h$ with $K_3 h$ and $K_4 h$. In the last curve, it is clear that the value of $K_1 h$ oscillates around the vertical line, $\mathrm{Re}\{Kh\} = \Gamma_1$.

The coalescence of the two modes implies that another new mode must be present, as occurs for example when double roots are obtained in the characteristic equation while solving an ordinary differential equation with constant coefficients. The new mode at the coalescence point is

$$e^{\pm iK_1 x}(\pm ix \cosh K_1(h+z) + (h+z)\sinh K_1(h+z)) \tag{5.7}$$

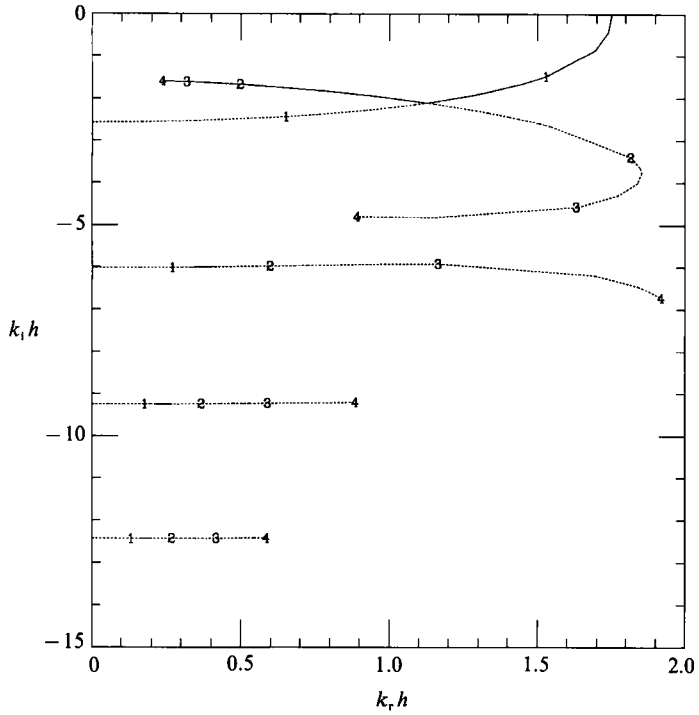

FIGURE 4. First five wavenumbers in the porous medium as the friction factor, f, varies from 0 to 4, for $\Gamma_1 = 1.6506$, showing the coalescence of the first two modes, K_1 and K_2. Solid line corresponds to K_1.

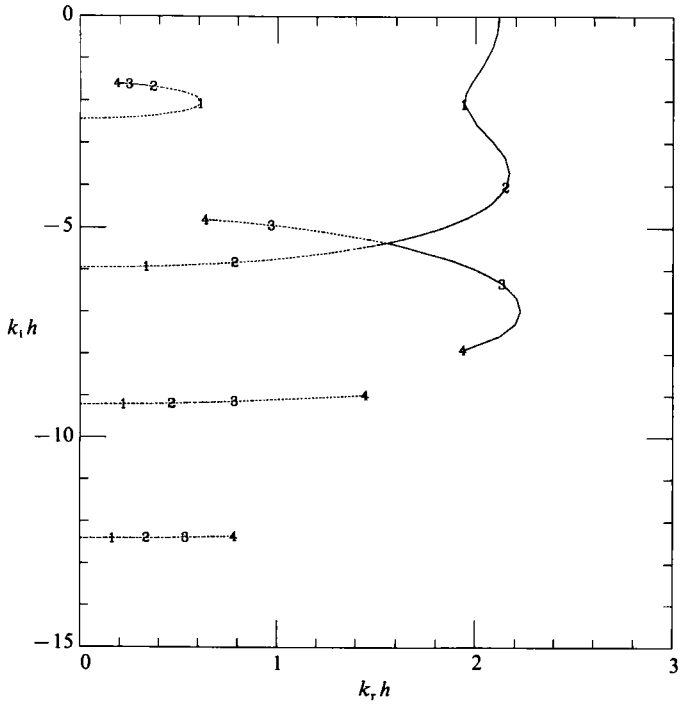

FIGURE 5. First five wavenumbers in the porous medium as the friction factor, f, varies from 0 to 4, for $\Gamma_1 = 2.0579$, showing the coalescence of K_1 and K_3. Solid line corresponds to K_1.

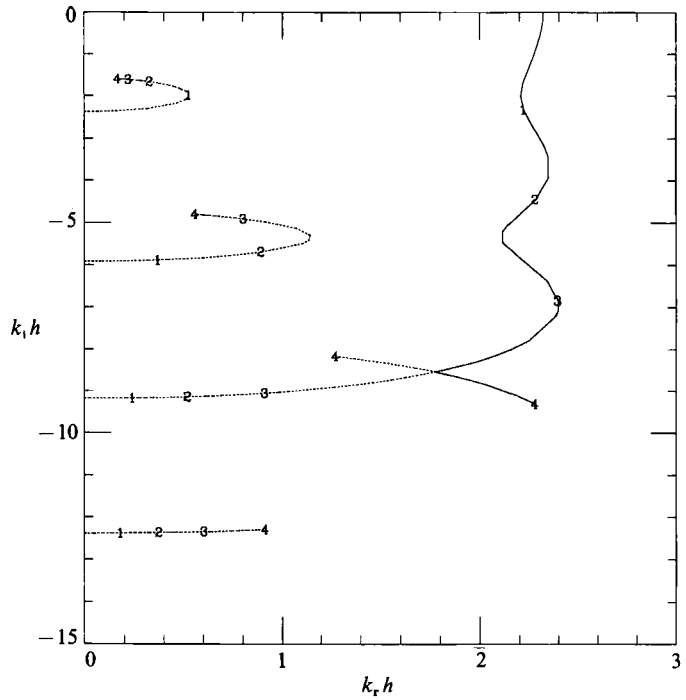

FIGURE 6. First five wavenumbers in the porous medium as the friction factor, f, varies from 0 to 4, for $\Gamma_1 = 2.2785$, showing the coalescence of K_1 and K_4. Solid line corresponds to K_1.

Mode	Kh	Γ_1	f
2	(1.12536, −2.10620)	1.65061	1.24801
3	(1.55157, −5.35627)	2.05785	2.59239
4	(1.77554, −8.53668)	2.27847	3.74051
5	(1.92940, −11.6992)	2.43112	4.80798
6	(2.04685, −14.8541)	2.54799	5.82647
7	(2.14189, −18.0049)	2.64270	6.81048

TABLE 1. Osculation points in the dispersion relationship

as shown in Appendix B using a Green's function approach. This mode coexists with the usual mode for this wavenumber,

$$\cosh K_1(h+z)\,\mathrm{e}^{\pm \mathrm{i}K_1 x}.$$

All of the originally (at $f = 0$) evanescent modes swap identities with K_1 at appropriate values of Γ_1 and f, as D' in (5.5) has an infinite number of roots, some of which are given in table 1. There are no triple roots, however, as D'' is never zero.

6. Results and conclusions

First, for a finite-width breakwater, we examine the reflection coefficient as a function of wave period (or depth) and the friction factor and wave direction. In figures 7 and 8, the magnitude of the reflection coefficient, $|R|$, is plotted versus $k_0 h$

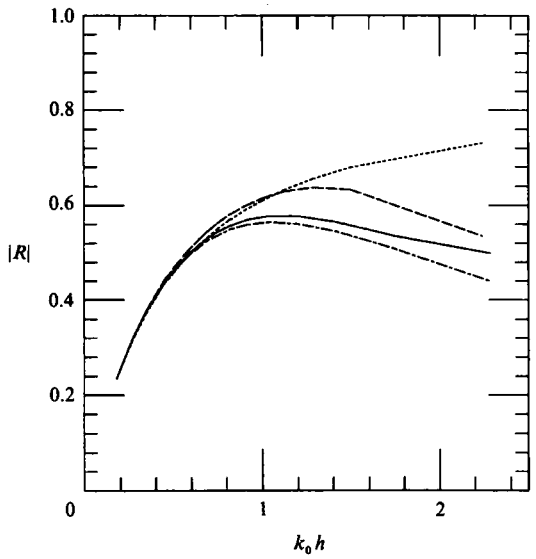

FIGURE 7. Reflection coefficient versus relative water depth for breakwater with $f = 1$, $b/h = 1$, $\theta = 0°$. Full long-wave model, ----; long-wave theory, (4.2), ——; plane-wave approximation; ——; full solution, ——.

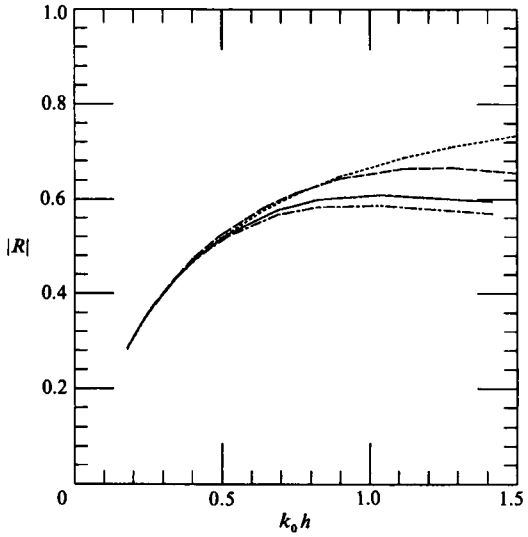

FIGURE 8. Reflection coefficient versus relative water depth for breakwater with $f = 1.5$, $b/h = 1$, $\theta = 0°$. Full long-wave model, ----; long-wave theory, (4.2), ——; plane-wave approximation, ——; full solution, ——.

for the various methods of solution with $b/h = 1$ for normal wave incidence. The complete solution (with 6 terms in the porous medium expansion) and the plane-wave approximation (4.2) are shown along with two long-wave approximations: the first with the wavenumbers chosen by the shallow-water relationships (4.4) and the second with the further approximation that $(K^2-\lambda^2)^{\frac{1}{2}}b \ll 1$ (O. Madsen 1974). This second long-wave model will be called the full long-wave model.

For figure 7, the friction factor is fixed as unity, $f = 1$, and for figure 8, $f = 1.5$. For

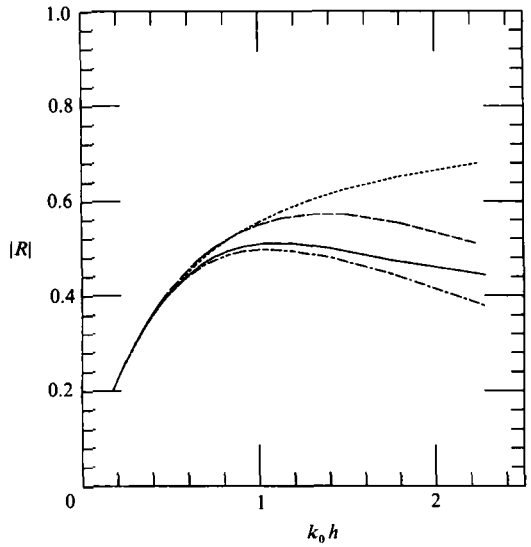

FIGURE 9. Reflection coefficient versus relative water depth for breakwater with $f = 1$, $b/h = 1$, $\theta = 30°$. Full long-wave model, ----; long wave theory, (4.2), ——; plane wave approximation, – – –; full solution, ——.

both figures, the full long-wave model diverges from the complete solution with increasing depth more rapidly than the other solutions. By comparing the two long-wave solutions, half of the error in the full long-wave model follows from the use of the incorrect dispersion relationship in intermediate-depth water and the other half from the assumption that the breakwater is short with respect to a wavelength. The plane-wave approximation diverges from the full solution in deeper water than the long-wave models and provides a reasonable estimate of the reflection coefficient for this case. For $k_0h < 1.5$, the relative error between the plane-wave approximation and the full solution is less than 5%. As the relative depth increases, the error becomes larger.

In figure 9, the wave angle of incidence is 30° and $f = 1$, which can be compared with figure 7, the normal incidence case. The non-zero wave angle results in smaller reflection coefficients for all methods (and correspondingly increased transmission coefficients). Again the plane-wave approximation works well for $k_0h < 1.5$.

As the friction factor increases, the plane-wave approximation begins to break down, as K_1 may no longer be the dominant progressive wave. For this reason, the plane-wave approximation in most cases should be restricted to small f-values, with 'small' depending on the value of dimensionless water depth Γ_1. The smaller this parameter, the larger f may be for the plane-wave approximation to still provide good estimates of R. For example, for $\Gamma_1 > 1.6501$ (corresponding to dimensionless depths greater than that necessary for the first coalescence of the wavenumbers in the porous medium), values of f less than one result in good (less than 10% error) estimates from the plane-wave theory, when compared to the complete solution. (Note that K_1 reaches a local minimum and K_2 reaches a maximum for $f \sim 1$ in figures 5 and 6.) However, in shallow water, for the case that $\Gamma_1 = 0.2012$, f can equal 10 with less than 2% error between the plane-wave approximation and the complete solution.

Figure 10 shows the magnitude of the reflection coefficient for the case of a rectangular breakwater with $b/h = 1$ for different (small) friction factors as a

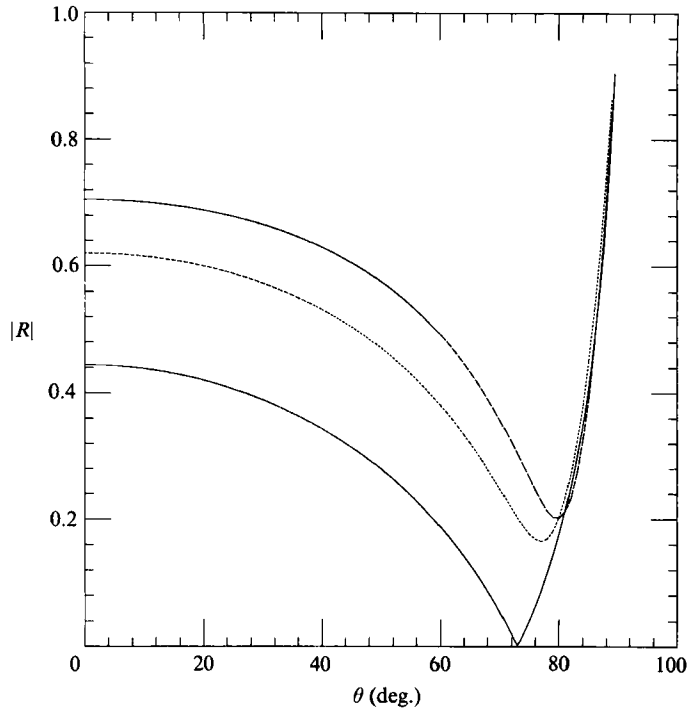

FIGURE 10. Reflection coefficient versus θ for breakwater with $b/h = 1$, $\omega^2 h/g = 0.2012$: $f = 1$, ——; $f = 3$, - - - -; $f = 5$, – – –.

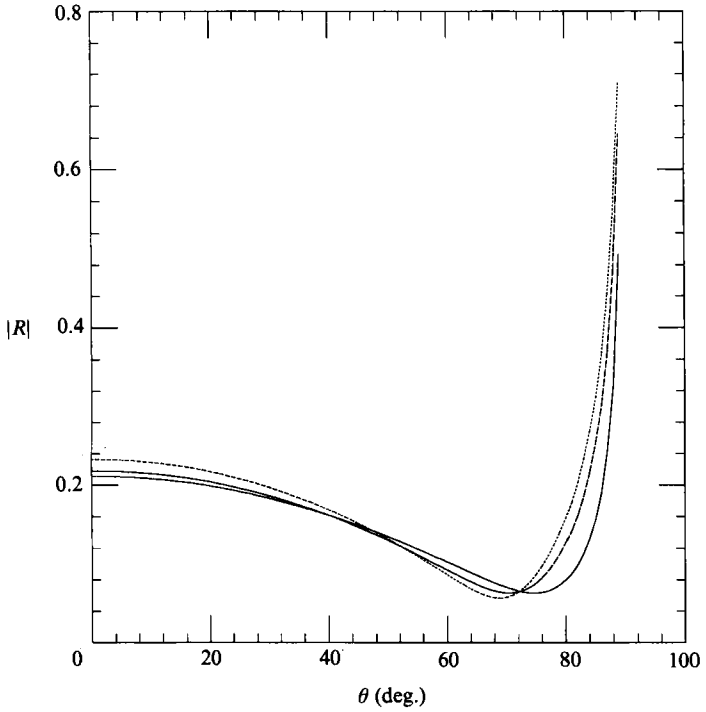

FIGURE 11. Reflection coefficient versus θ for breakwater with $b/h = 1$, $\omega^2 h/g = 1.6010$: $f = 0.25$, ——; $f = 0.5$, - - - -; $f = 0.75$, – – –.

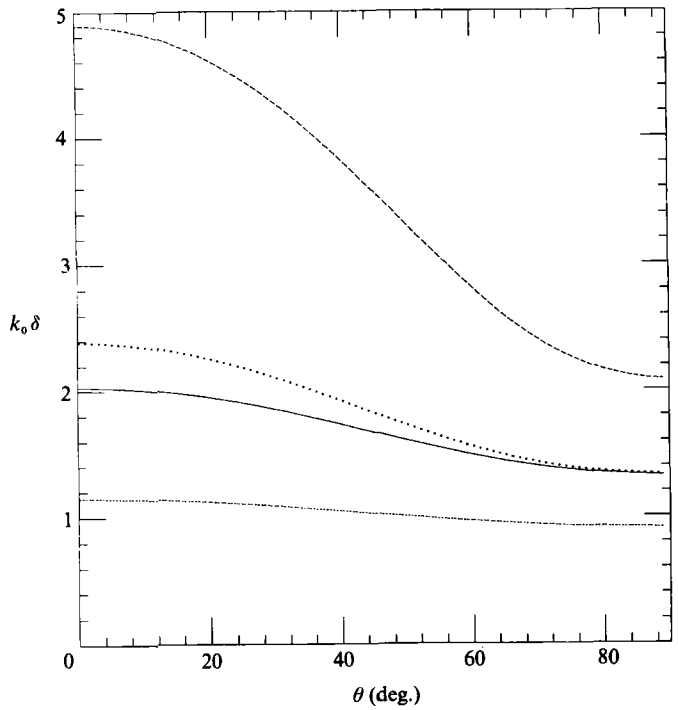

FIGURE 12. Dimensionless skin depth versus θ for a semi-infinite breakwater for two dimensionless water depths and f-values. For $\Gamma_1 = 0.2012$: $f = 1$, ——; $f = 2$, ·····. For $\Gamma_1 = 1.6010$: $f = 0.25$, ----; $f = 0.5$, · · · ·.

function of angle of incidence, using the plane-wave approximation. If the friction factor is high, the reflection coefficient is generally larger than the case for a breakwater with a smaller friction factor. Figure 11 shows the same variables but for deeper water.

The minimum in the reflection coefficient, which occurs for large angles is shown in this figure, corresponds approximately to a maximum in the transmission coefficient. This minimum occurs at different angles of incidence as f (or m) changes (and, for small $b(K^2-\lambda^2)^{\frac{1}{2}}$ is independent of the width of the breakwater). This case is similar to the non-dissipative case of waves incident on a submerged obstacle or a step change in water depth. For the case of a small submerged obstacle, Miles (1981) has shown that the reflection coefficient is zero for 45° incidence regardless of the shape of the bottom obstacle. For a step, which is analogous to the case of the reflection and transmission of light from two dissimilar media, a zero reflection coefficient occurs at the *Brewster angle*, which can be shown to occur at $\tan\theta_b = k_1/k_2$ in the long-water-wave analogy. The explanation for no reflection in optics is that the transmitted wave direction is at a 90° angle to the reflected wave angle. Therefore there can be no energy transferred into the reflected wave mode. If one of the two media is dissipative, such as the case of electromagnetic waves impinging on a conductor, which is analogous to our present topic, the minimum in the reflection coefficient is known as the *principal angle of incidence*, Mathieu (1975).

For an infinitely wide structure, the oscillations induced by the incident waves decay with distance into the structure. A measure of this decay is the *skin depth*, which is the distance over which the motion has decayed to e^{-1}. We non-

dimensionalize the skin depth δ with the wavenumber k_0 and define it for the plane-wave approximation as

$$k_0\delta = \frac{k_0}{(K_1^2-\lambda^2)^{\frac{1}{2}}}. \tag{6.8}$$

It is shown versus incident angle in figure 12 for $\Gamma_1 = 0.2012$, and 1.6010, each with two values of f. For all cases the penetration into the structure is reduced for larger f-values and with increasing angles of incidence. Furthermore, the skin depth is less than the wavelength ($2\pi/k_0$) for all cases, so that structures wider than a wavelength can be considered semi-infinite structures.

The first author acknowledges support by the NOAA Office of Sea Grant, Department of Commerce, under Grant NA87AA-D-SG040 and appreciates helpful comments by James T. Kirby. The second author thanks the Fulbright Program for support for a stay during 1988–1989 at the University of Delaware and the Comision Asesora Cientifica y Técnica for support under Grant PA85-0176.

Appendix A. Equations in the porous medium

In order to describe the wave field inside a breakwater of porosity ϵ, it is necessary to describe the fluid motion of the incompressible fluid in the pores of the rigid structure in terms of the seepage velocity vector, $\boldsymbol{q}$, which has components in all three coordinate directions, and the pore pressure, p. These quantities are obtained by averaging over a finite volume, containing both the solid phase of the porous medium and the pores.

Following Sollitt & Cross (1972), the conservation-of-mass equation can be expressed as

$$\nabla \cdot \boldsymbol{q} = 0.$$

The equation of motion includes resistance forces described by Forchheimer's model and an additional term which evaluates the added resistance caused by the added mass of discrete grains within the porous medium (Sollitt & Cross 1972; Hannoura & McCorquodale 1978). This equation may be written as

$$s\frac{\partial \boldsymbol{q}}{\partial t} = -\nabla\left(\frac{p}{\rho_w}+gz\right)-\left[\frac{\nu}{R_p}+\frac{C_f\epsilon}{R_p^{\frac{1}{2}}}q\right]\epsilon\boldsymbol{q}, \tag{A 1}$$

where $q = |\boldsymbol{q}|$ and the fluid has density ρ_w and kinematic viscosity ν. Two hydraulic properties of the porous medium used in this equation are the intrinsic permeability, R_p and the turbulent resistance coefficient, C_f; s is an inertial coefficient, defined by

$$s = 1+\frac{1-\epsilon}{\epsilon}C_M, \tag{A 2}$$

where C_M is the added-mass coefficient of the grains. The parameter s is often taken as unity in practice, although Le Méhauté (1957) and Sulisz (1985) report better correlations with laboratory data with values approaching 2. Here we have taken s to be unity.

Assuming time-periodic motion, with the same angular frequency as the waves, ω, this equation may be linearized on the basis of Lorentz's hypothesis of equivalent work, replacing the dissipative nonlinear stress term in (A 1) by an equivalent linear

term, $f\omega\boldsymbol{q}$, where f is a dimensionless friction coefficient. This yields the linearized form of the equation,

$$is\omega\boldsymbol{q} = -\boldsymbol{\nabla}\left(\frac{p}{\rho_w}+gz\right)-\omega f\boldsymbol{q}. \tag{A 3}$$

Taking the curl of this equation shows that the flow in the porous medium is irrotational and can be described by a potential, $\boldsymbol{q} = \boldsymbol{\nabla}\Phi$. Substituting the potential into (A 3) results in a Bernoulli equation within the porous medium:

$$s\frac{\partial\Phi}{\partial t}+\frac{p}{\rho_w}+gz+f\omega\Phi = 0. \tag{A 4}$$

Finally, substituting the potential into the conservation-of-mass equation yields Laplace's equation, which must hold everywhere within the medium.

At the phreatic surface, the Bernoulli equation can be combined with the linear kinematic condition that the water particles in the surface follow the surface,

$$\frac{\partial\eta}{\partial t} = \frac{\partial\Phi}{\partial z},$$

to yield

$$\frac{\partial\Phi}{\partial z}-\omega^2(s-if)\frac{\Phi}{g} = 0. \tag{A 5}$$

Solutions to these equations depend on the values of s, ϵ, f, C_f and R_p, which are related to the type of porous structure considered and are taken as given. However, to evaluate the linearized friction coefficient, f, an additional condition is required. Following others, the Lorentz's hypothesis of equivalent work has been assumed. In doing this, f is evaluated from the following equation:

$$f\omega = \frac{\displaystyle\int_0^L \mathrm{d}y\int_{-h}^0 \mathrm{d}z\int_0^b \mathrm{d}x\int_0^T \epsilon\left[\frac{\nu}{R_p}+\frac{C_f\epsilon}{R_p^{\frac{1}{2}}}q\right]q^2\,\mathrm{d}t}{\displaystyle\int_0^L \mathrm{d}y\int_{-h}^0 \mathrm{d}z\int_0^b \mathrm{d}x\int_0^T q^2\,\mathrm{d}t}, \tag{A 6}$$

where $L = 2\pi/\lambda$. The determination of f is therefore iterative, as f is required to determine the q.

Here, however, f is taken as a given constant, which, in principle, could range from zero to infinity; for porous breakwaters, it is of $O(1)$, while for wave absorbers in wave tanks it can be higher.

Appendix B. Green's function approach

The eigenfunction expansion can be found through the use of a Green's function, which will be shown for the porous medium, where the presence of a double pole affects the solution for discrete values of the parameter, $\Gamma_2 = \omega^2 h(s-if)/g$. First the simple-pole case will be treated.

The Green's function for the velocity potential at (x, z) due to a wave source at (ξ, ζ) is given by John (1950, p. 99), for $z < \zeta$, as

$$G(x, z; \xi, \zeta) = -\int_0^\infty p(\mu)\frac{\cos\mu(x-\xi)}{\mu}\,\mathrm{d}\mu, \tag{B 1}$$

where
$$p(\mu) = 2\cosh\mu(h+z)\left\{\frac{\mu h\cosh\mu\zeta + \Gamma_2\sinh\mu\zeta}{\mu h\sinh\mu h - \Gamma_2\cosh\mu h}\right\}. \tag{B 2}$$

For $f > 0$, $p(\mu)$ has poles in the second and fourth quadrants; note that $p(\mu) = -p(-\mu)$. Write (B 1) as the sum of two integrals, using

$$2\cos\mu(x-\xi) = \mathrm{e}^{\mathrm{i}\mu|x-\xi|} + \mathrm{e}^{-\mathrm{i}\mu|x-\xi|}. \tag{B 3}$$

Deform the contour in the first (second) integral into the positive (negative) imaginary axis. There is no contribution from the large quarter-circles, in the limit, by Jordan's lemma. The two contributions from integrating along the imaginary axis cancel. This leaves only the residue contributions to the second integral. Evaluating these residues at the simple poles, ($\mu = K_m$), where K_m are the (complex) roots of

$$D(K_m) \equiv K_m h\sinh K_m h - \Gamma_2\cosh K_m h = 0, \tag{B 4}$$

with $\mathrm{Re}\,(K_m) > 0$ and $\mathrm{Im}\,(K_m) < 0$, yields

$$G(x,z;\xi,\zeta) = 4\pi\mathrm{i}\sum_m \frac{\cosh K_m(h+z)\cosh K_m(h+\zeta)\,\mathrm{e}^{-\mathrm{i}K_m|x-\xi|}}{2K_m h + \sinh 2K_m h}, \tag{B 5}$$

showing that the eigenfunctions are of the form

$$\cosh K_m(h+z)\,\mathrm{e}^{\pm\mathrm{i}K_m x}. \tag{B 6}$$

For those cases where double poles exist, that is, when K_1 coalesces with a K_m and both $D(K_1)$ and $D'(K_1)$ are zero, the residue of $P(\mu)/D(\mu)$ is (see e.g. Churchill 1960)

$$\frac{2P'}{D''} - \frac{2}{3}\frac{PD'''}{(D'')^2}, \tag{B 7}$$

where $D(\mu)$ is as before and

$$P(\mu) = h\left(\cosh\mu\zeta + \frac{\Gamma_2}{\mu}\sinh\mu\zeta\right)\cosh\mu(h+z)\,\mathrm{e}^{-\mathrm{i}\mu|x-\xi|}. \tag{B 8}$$

Thus, we find that a double pole at K_1 contributes to the expansion of G a term

$$\frac{2\pi\mathrm{i}Q(z,\zeta)}{h\cosh^2 K_1 h}\,\mathrm{e}^{-\mathrm{i}K_1|x-\xi|}, \tag{B 9}$$

where

$$\begin{aligned} Q(z,\zeta) = {} & [-\mathrm{i}|x-\xi|\cosh K_1(h+z) + (h+z)\sinh K_1(h+z)]\cosh K_1(h+\zeta) \\ & + [-\tfrac{4}{3}h\cosh K_1(h+\zeta)\tanh K_1 h + (h+\zeta)\sinh K_1(h+\zeta)]\cosh K_1(h+z). \end{aligned} \tag{B 10}$$

This shows that the appropriate eigenfunctions at K_1 are of the form

$$\{\pm\mathrm{i}x\cosh K_1(h+z) + (h+z)\sinh K_1(h+z)\}\,\mathrm{e}^{\pm\mathrm{i}K_1 x} \quad \text{and} \quad \cosh K_1(h+z)\,\mathrm{e}^{\pm\mathrm{i}K_1 x}. \tag{B 11}$$

REFERENCES

Churchill, R. V. 1960 *Complex Variables and Applications*. McGraw-Hill.

Craik, A. D. D. 1985 *Wave Interactions and Fluid Flows*. Cambridge University Press.

Dattatri, J., Raman, H. & Shankar, J. N. 1978 Performance characteristics of submerged breakwaters. In *Proc. 16th Coastal Engng Conf., Hamburg*, pp. 2153–2171. ASCE.

Hannoura, A. A. & McCorquodale, I. A. 1978 Virtual mass of coarse granular media. *J. Waterways, Ports, Coastal Ocean Engng Div., ASCE* **104**, 191–200.

IWASAKI, T. & NUMATA, A. 1970 Experimental studies on wave transmission of a permeable breakwater constructed by artificial blocks. *Coastal Engng Japan* **13**, 25–29.

JOHN, F. 1950 On the motion of floating bodies, II. *Commun. Pure Appl. Maths* **3**, 45–101.

LE MÉHAUTÉ, B. 1957 Perméabilité des digues en enrochements aux ondes de gravité périodiques. *Houille Blanche* **6**, 903–919.

MADSEN, O. S. 1974 Wave transmission through porous structures. *J. Waterways, Ports, Coastal Ocean Engng Div., ASCE* **100**, 169–188.

MADSEN, O. S. & WHITE, S. M. 1976 Wave transmission through trapezoidal breakwaters. In *Proc. 15th Coastal Engng Conf., Honolulu*, pp. 2662–2676. ASCE.

MADSEN, P. A. 1983 Wave reflection from a vertical permeable wave absorber. *Coastal Engng* **7**, 381–396.

MATHIEU, J. P. 1975 *Optics*. Pergamon.

MILES, J. W. 1981 Oblique surface-wave diffraction by a cylindrical obstacle. *Dyn. Atmos. Oceans* **6**, 121–123.

MORSE, P. M. & INGARD, K. U. 1968 *Theoretical Acoustics*. Princeton University Press.

SOLLITT, C. K. & CROSS, R. H. 1972 Wave transmission through permeable breakwaters. In *Proc. 13th Coastal Engng Conf., Vancouver*, pp. 1827–1846. ASCE.

SOLLITT, C. K. & CROSS, R. H. 1976 Wave reflection and transmission at permeable breakwaters. *Tech. Paper* 76-8. US Army Corps of Engineers, Coastal Engineering Research Center.

SULISZ, W. 1985 Wave reflection and transmission at permeable breakwaters of arbitrary cross section. *Coastal Engng* **9**, 371–386.

TESTER, B. J. 1973 The optimization of modal sound attenuation in ducts, in the absence of mean flow. *J. Sound Vib.* **27**, 477–513.

YEH, P. 1988 *Optical Waves in Layered Media*. John Wiley & Sons.